Assessment of MaMIMO beamwidth using measurements and raytracing
Évaluation des ouverture de faisceau MaMIMO à l'aide de mesures et de raytracing

Maarten Velghe[1], Sergei Shikhantsov[1], Luc Martens[1], Wout Joseph[1] and Arno Thielens[1]

[1]Department of Information Technology, Ghent University/IMEC, Technologiepark 126, 9052 Ghent, Belgium

MaMIMO, beamwidth, RF-EMF exposure / *MaMIMO, ouverture de faisceau, exposition RF-EMF*

Abstract/Résumé

The width of a beam produced by MaMIMO arrays will affect a user's exposure to RF-EMFs. We performed measurements in an anechoic chamber using a virtual arrays and successfully assessed this beamwidth. We validated our measurements with simulations.

L'ouverture d'un faisceau produit par les réseaux MaMIMO affectera l'exposition d'un utilisateur aux RF-EMF. Nous avons effectué des mesures dans une chambre anéchoïque avec des réseaux virtuels et évalué cette ouverture de faisceau. Nous avons validé nos mesures avec des simulations.

1 Introduction

In the fifth generation of telecommunication networks, Massive Multiple-input-multiple-output (MaMIMO, [1]) base stations (BSs) will produce narrow RF-EMF beams aimed at each specific user device they service. Knowledge on the widths of these beams is essential to evaluate a user's exposure to RF-EMFs. The aim of this study is to assess this beamwidth via measurements in an anechoic chamber and to validate the used setup with free-space simulations.

2 Materials and Method

2.1 Measurement setup

Figure 1 shows a schematic top view of the measurement setup in the anechoic chamber. Two vertically polarized dipole dual cone broadband antennas, a transmitting (TX) and receiving (RX) antenna, are connected to a vector network analyser (VNA) performing measurements at 3.5 GHz. The TX antenna is fixed on a linear positioning system, moving along the y-axis. The RX antenna is placed on a 2D positioning system, consisting of two orthogonally oriented linear positioners moving along the y- and x-axis. Positioning systems are co-planar, such that the antennas stay in the same xy-plane as they move.

The TX grid has 17x1 locations, with the interspacing chosen to be δ_{Tx}=4.28 cm, which is about half the wavelength. This results in an array aperture L of 68 cm. The TX-RX distance D is chosen to be 68 cm as well. The RX grid has 33x17 locations (33 elements along the y-axis per 17 elements along the x-axis) with an interspacing half of the TX interspacing (δ_{Rx}=2.14 cm). We measure the channel transfer function $h_{kn,measured}$ between each Tx-position k (k=1…17) and each Rx-position n (n=1…561), resulting in the channel matrix $\mathbf{H}_{measured}$.

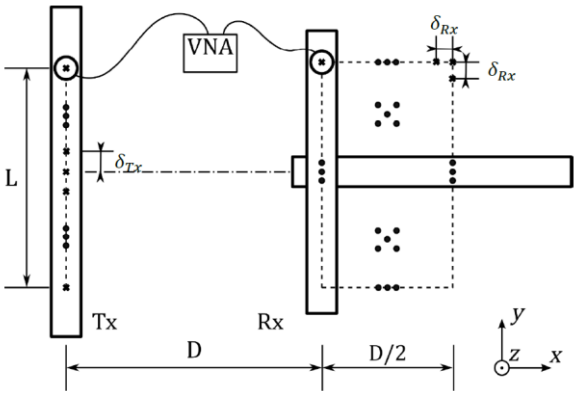

Figure 1: Schematic overview of the measurement setup.

To validate the measurement results, we estimate the wireless channel between the TX and RX virtual arrays using a Line-of-Sight (LOS) propagation model. This is suitable for calculating propagation in the anechoic chamber with virtual arrays, as it only takes into account direct propagation paths between TX-RX pairs and neglects mutual coupling effects of the arrays' antennas. This results in the simulated channel matrix $\mathbf{H}_{\mathbf{model}}$.

2.2 Post processing

The channel correlation matrix (CM) is commonly used for the analysis of the performance of MaMIMO systems is defined as

$$\mathbf{G} = \mathbf{H}^{*}\mathbf{H}. \tag{1}$$

This results in two 561x561 CMs: $\mathbf{G}_{\mathbf{measured}}$ and $\mathbf{G}_{\mathbf{model}}$ which are complex valued with real values on the main diagonal. To simplify the analysis we take the average of the results in each of the 17 Rx-rows along the x-axis. This way we calculate the average beamwidth over the distance x=[68cm 102cm]. This results in the 33x33 averaged CMs $\mathbf{G}_{\mathbf{avg,measured}}$ and $\mathbf{G}_{\mathbf{avg,model}}$. These are normalized to

To assess the beamwidth, we define the spatial correlation function (CF) $\rho(\mathbf{G}_{\mathbf{avg}}, \mathrm{i})$ as the average over the i^{th} diagonal of $\mathbf{G}_{\mathbf{avg}}$:

$$\rho(\mathbf{G}_{\mathbf{avg}}, \mathrm{i}) = \frac{\sum_{\mathrm{k}=1}^{33-\mathrm{i}} \left| g_{\mathrm{k,k+i}} \right|}{33 - \mathrm{i}}, \tag{2}$$

with g_{lm} an element of $\mathbf{G}_{\mathbf{avg}}$. ρ can be treated as a function of the distance in the y-direction between the receivers.

The average relative difference σ_{avg} between $\mathbf{G}_{\mathbf{avg,measured}}$ and $\mathbf{G}_{\mathbf{avg,model}}$ is calculated as

$$\sigma_{\mathrm{avg,lm}} = \left| \frac{\left| g_{\mathrm{avg,model,lm}} \right| - \left| g_{\mathrm{avg,measured,lm}} \right|}{\frac{\left| g_{\mathrm{avg,model,lm}} \right| + \left| g_{\mathrm{avg,measured,lm}} \right|}{2}} \right|, \tag{3}$$

with $\sigma_{avg,lm}$ an element of σ_{avg}.

3 Results and Discussion

Figure 2 compares $\rho(\mathbf{G}_{\mathbf{avg,model}})$ and $\rho(\mathbf{G}_{\mathbf{avg,measured}})$. A very good agreement is observed. Both functions have maximum at $\delta y=0$ and decrease rapidly within a 1-wavelength distance (8.57 cm). After minor oscillations they flatten-out at around 4% of their maximum value for $\delta y>0.5$ m ($\approx 6*\lambda$).The distance between the maximum and half the maximum $\delta_{hm}y=6.5$ cm, the beamwidth is thus $2*\delta_{hm}y=13$ cm.

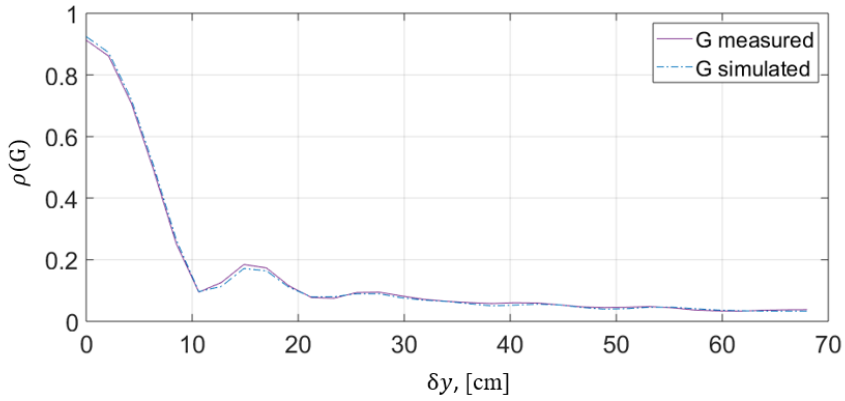

Figure 2: Spatial correlation function of $G_{avg,measured}$ and $G_{avg,model}$ in terms of the distance between their rows.

In Figure 3 the normalized CMs $\mathbf{G}_{\mathbf{avg,measured}}$ (3a), $\mathbf{G}_{\mathbf{avg,model}}$ (3b) and their difference σ_{avg} (3c) are shown. The main diagonal dominance is apparent in both averaged CMs. The same result has been obtained in measurement campaigns [2] and using geometry-based models [3]. σ_{avg}, does not exceed 5% on the main diagonal. This implies a good agreement between measurements and simulations. However, some of the out-of-diagonal

elements exceed 30%. The reason for that are the low absolute correlation values observed at large RX separation distances, which are shown in the top-right corner of the CMs. Even a small variation of the received signal (due to e.g. reflections by the positioners and support structures, alignment errors, radiation pattern variation) results in a relatively high simulation error.

This measurement setup can now be used to evaluate exposure from MaMIMO systems in other environments, such as a room without absorbing materials, with obstructed line-of-sight conditions, etc.

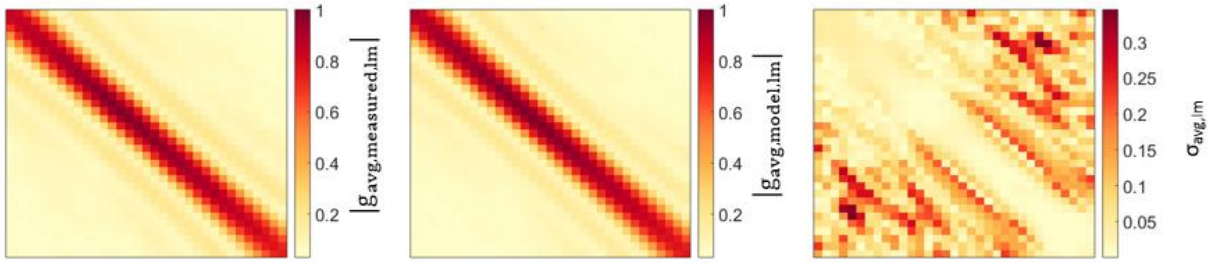

(a) *(b)* *(c)*

Figure 3: The normalized correlation matrices $G_{avg,measured}$ (a), $G_{avg,model}$(b), and their relative difference σ_{avg} (c).

4 Conclusion

We measured and simulated the beamwidth of a MaMIMO array and found $2*\delta_{hm}y$=13 cm. A good agreement between measurements and simulations was observed.

References

[1] Marzetta, et al. 2010. *IEEE Trans. Wirel. Commun.*, 9(11): 3590.

[2] Claessens, et al. 2018. *IEEE International Workshop on SPAWC*, 19: 1–5.

[3] Marzetta, 2016. *Fundamentals of Massive MIMO*. Cambridge University Press.

COMITÉ NATIONAL FRANÇAIS DE RADIOÉLECTRICITÉ SCIENTIFIQUE
UNION RADIO SCIENTIFIQUE INTERNATIONALE
SIÈGE SOCIAL : ACADÉMIE DES SCIENCES, 23 QUAI DE CONTI, PARIS 6ÈME

JOURNÉES SCIENTIFIQUES, *WORKSHOP*

RÉSEAUX DU FUTUR : 5G ET AU-DELÀ

FUTURE NETWORKS: 5G AND BEYOND

11 / 13 MARS, 2020

TELECOM PARIS, INSTITUT POLYTECHNIQUE DE PARIS, PALAISEAU

ACTES *PROCEEDINGS*